

HALO FORMATION OF THE HIGH INTENSITY BEAMS IN A PERIODIC SOLENOID FOCUSING FIELDS*

Y. L. Cheon[†], M. Chung

Ulsan National Institute of Science and Technology, Ulsan, Korea

Abstract

Transport of high-intensity beams over long distances can be restricted by space-charge fields which can lead to the beam emittance growth and particle losses in accelerators. The lost particles cause serious radioactivation of the accelerator structure and disturb the proper propagation of the beam. The space-charge fields can be calculated by using Poisson's equation from the charge density profile. There are several ways to focus the charged particles in accelerators, but we are going to consider a periodic solenoidal magnetic focusing field. For the Kapchinskij-Vladimirskij (K-V) beams, the space charge field is linear but the envelope can be mismatched and have parametric resonances of the envelope instabilities particularly in periodic solenoid fields. The perturbed oscillations of the core and test particles can generate resonances following by the halo formations. Also, charge non-uniformity can make halos because of the non-linear space charge force.

INTRODUCTION

High-intensity charged particle beams can be used in various kinds of research like astrophysical nuclear reaction experiments, finding new particles in a standard model, application for cancer treatment and fusion material test such as International Fusion Materials Irradiation Facility (IFMIF). During the transport of the high-intensity beams which are space charge dominated, halo particles can be generated by the envelope mismatch [1] or the non-uniformities of charged particle distributions [2, 3]. We are going to describe the halo formations of uniform density beams whose core is not matched, and Gaussian density beams on the matched condition. To do that, in this paper, we just deal with the periodic solenoidal focusing field which has advantages over other focusing methods that it's much simpler and cheaper in the experimental aspect, rotationally symmetric, and more efficient in terms of beam emittance control [4]. Also it is more suitable for the numerical analysis using the smooth approximation [5, 6].

TRANSVERSE BEAM DYNAMICS UNDER A PERIODIC SOLENOID FOCUSING

A longitudinal solenoid focusing function can be expressed by $\kappa_z(s) = \kappa_z(s + S) = q^2 B_z^2(s) / 4\gamma_b^2 \beta_b^2 m^2 c^4$, where $B_z(s) = B_z(0, s)$ is the magnetic field on the z axis, S is the period of the focusing field. For a simple model, it's

assumed that $\kappa_z(s) = \kappa_z(0) = \text{const.}$ when $0 \leq s \leq \frac{\eta}{2}S$ & $S(1 - \frac{\eta}{2}) \leq s \leq S$, and $\kappa_z(s) = 0$ when $\frac{\eta}{2} \leq s \leq S(1 - \frac{\eta}{2})$ [5].

Envelope Equation

With the dimensionless parameters and variables defined by $s/S \rightarrow s, r_b/\sqrt{\epsilon S} \rightarrow r_b, S^2 \kappa_z \rightarrow \kappa_z$, and $SK/\epsilon \rightarrow K$, the normalized envelope equation for a symmetric envelope radius r_b becomes [5–8]

$$\frac{d^2 r_b(s)}{ds^2} + \kappa_z(s) r_b(s) - \frac{K}{r_b(s)} - \frac{1}{r_b^3(s)} = 0, \quad (1)$$

where ϵ is the beam emittance and $K = 2q\lambda/\gamma_b^3 \beta_b^2 mc^2$ is the normalized beam perveance in which λ is the line charge density of the beam. The normalized vacuum phase advance over one axial period of such a focusing field is given approximately by $\sigma_0 = \int_0^1 \sqrt{\kappa_z(s)} ds = \sqrt{\eta \kappa_z(0)}$, and normalized depressed phase advance which is considered as the degree of the space charge force is given by $\sigma = \int_0^1 \frac{ds}{r_b^2(s)}$.

Equation of Motion of a Charged Particle

In order to use the particle-core model for the study of halo formations, we will only deal with the transverse particle motions in the transverse phase space (x, y directions) and neglect the longitudinal effects (z or s direction) of space charge force and acceleration of the particles.

The dynamics of charged particles in the simple solenoid focusing model is easily analyzed in the Larmor frame [9] which rotates with the Larmor frequency around the axis of the solenoid. In Larmor frame, the equation of motion of a charged particle, with the space charge force (F_{sc}) is

$$x''(s) + \kappa_z(s)x(s) - KF_{sc}(x, r_b) = 0, \quad (2)$$

where $F_{sc}(x, r_b) = x(s)/r_b^2(s)$ for $x(s) < r_b(s)$ and $1/x(s)$ for $x(s) > r_b(s)$ for the uniform density beams.

However in real frame, with nonzero canonical angular momentum of the particles, the generalized equations of motion of a charged particle under the periodic solenoid field can be expressed by [9]

$$x''(s) - 2\sqrt{\kappa_z(s)}y'(s) - \frac{K}{2}F_{sc,x}(x, y) = 0, \quad (3)$$

$$y''(s) + 2\sqrt{\kappa_z(s)}x'(s) - \frac{K}{2}F_{sc,y}(x, y) = 0, \quad (4)$$

which are coupled between x and y directions and the longitudinal acceleration term (γ') is neglected. For simple case of zero canonical angular momentum, the coupled equations become a simple form in radial direction r, which is

$$r''(s) + \kappa_z(s)r(s) - \frac{K}{2}F_{sc,r}(r) = 0. \quad (5)$$

* Work supported by the National Research Foundation of Korea (Grant No. NRF-2017M1A7A1A02016413)

[†] mchung@unist.ac.kr

ENVELOPE OSCILLATIONS

In this section, we will see the envelope instabilities that explore mismatched, nonlinear resonances and chaotic behaviors in the beam envelope oscillations [5].

With solving Eq.(1), we plotted the envelope oscillations in phase plane $r_b - r'_b$, with different values of space charge perveance and focusing parameters. All points in the figures are plotted in every S lattice period (Poincare surface of section plots) for the trajectories of many different envelope initial conditions for propagation over 300 lattice periods.

Figure 1 shows the envelope motions without the space charge term, i.e, $K = 0$. The values of normalized parameters correspond to $\eta = 1/6, \kappa_z(0) = 3.79(\sigma_0 = 45.5^\circ)$. As you can see in the figure, there's a fixed point on the phase plane which represents the matched beam. It corresponds to a periodic solution to the envelope equation in every lattice period and the corresponding initial condition is $r_b(0) = 1.16, r'_b(0) = 0$. Around the fixed point, there are infinite number of invariant tori, each of which describes a mis-matched beam whose envelope exhibits stable betatron oscillations about the envelope of the matched beam because of the initial mismatch.

On the other hand, with non zero perveance, the space charge effects induce parametric resonances as well as the matched and mismatched oscillations as shown in Fig.2. Here, the values of normalized parameters correspond to $K = 3, \eta = 1/6, \kappa_z(0) = 3.79(\sigma_0 = 45.5^\circ)$ and the initial condition of a fixed point is $r_b(0) = 2.3, r'_b(0) = 0$. There coexist 4-th and 5-th order resonances in this phase space. The 5-th order resonance corresponds to the five elliptical regions in the vicinity of the fixed point. It has betatron wave number of $2\pi/5$, so a trajectory in one of the five islands will hop from one to another island until it comes back to its starting point after five turns [10].

For sufficiently large perveance values, the envelope oscillations become chaotic for some mismatched conditions. The phase space contains chaotic orbits which are very sensitive to initial conditions [5].

HALO FORMATIONS IN A PARTICLE CORE MODEL

From now, we will see the halo formations of charged particles in the particle-core model.

Halo formation of high-intensity beams which are space charge dominated can lead to beam emittance growth and particle losses in accelerators [11–14], and there are many reasons for the halos during the beam transport.

- Envelope instabilities related to the mis-matched and the n-th order parametric resonances (in the previous section).
- Halo formations generated by the resonances between the core oscillation and that of test particles (Particle-Core model) [1, 2, 15–17].
- Charge non-uniformity that induce the non-linear space charge force [3, 18].

We are going to describe the halo formations and chaotic motions both in the uniform charge density beams that are not matched, and non-uniform (Gaussian) charge density beams that are matched in the solenoid focusing field. To do that, we solved the equations of motion in our simulation to understand the motions between the core and test particles.

Particle Core Model of Uniform Density Beams

By solving Eq.(2) for the uniform density beam, the trajectories of many test particles with different initial positions are plotted in the phase plane in every lattice period for propagation over 300 lattice periods (see Fig.3).

Figure 3(a) shows the motion of test particles in the case of matched beam. They have stable circular or elliptical orbits in the phase space. But in the case of the mis-matched beam [see Fig.3(b)], we can see irregular trajectories around the center and chaotic motions that move in and out of the central region. Particularly, for the 5-th order resonant instability [see Fig.3(c)], particles are plotted in every 5 lattice period because such core oscillations have $2\pi/5$ frequency and return to the starting point every 5 lattice period. We can see resonant trajectories symmetrically generated in the space.

Outside the beam boundary, particles experience a nonlinear force proportional to $1/x$ and it is independent of the size of the beam. But when the test particles pass through the beam core, they are decelerated by the space charge force as they approach the core and accelerated as they leave the core. Also the space charge force within the beam boundary is dependent of the size of the envelope radius. Therefore, the unstable core oscillations like mis-matched and n-th order parametric resonances induce non-linear space charge forces to the charged particles and generate resonances accompanied by the chaotic and halo formations.

Particle Core Model of Gaussian Density Beams

$$\rho(\vec{x}) = \frac{\lambda}{2\pi\sigma_x\sigma_y} \exp\left(-\frac{x^2}{2\sigma_x^2} - \frac{y^2}{2\sigma_y^2}\right) \quad (6)$$

If a charge density of the beam has Gaussian distribution [Eq.(6)], the corresponding electric fields calculated by Poisson's equation are [19, 20]

$$E_{sc,x}(x, y) = 2\lambda \frac{1 - e^{-r^2/\sigma_r^2}}{r^2} x, \quad (7)$$

$$E_{sc,y}(x, y) = 2\lambda \frac{1 - e^{-r^2/\sigma_r^2}}{r^2} y, \quad (8)$$

where $r^2 = x^2 + y^2$. In this equation, σ_r is the rms radial size of the Gaussian profile and it corresponds to $\sigma_r = \sigma_r(s) = r_b(s)/\sqrt{2}$, where $r_b(s)$ is the envelope radius coming from the initial condition of the matched beam by solving the Eq.(1). $r_b(s)/\sqrt{2}$ is the rms size of the matched beam with uniform density profile and it's same with $\sigma_r(s)$ based on the concepts of **Equivalent beams** [9]. Therefore, Eqs.(7) and (8) can be substituted into the Eq.(3) and (4) so that the space charge terms become $F_{sc,x} = E_{sc,x}/\lambda$ and $F_{sc,y} = E_{sc,y}/\lambda$.

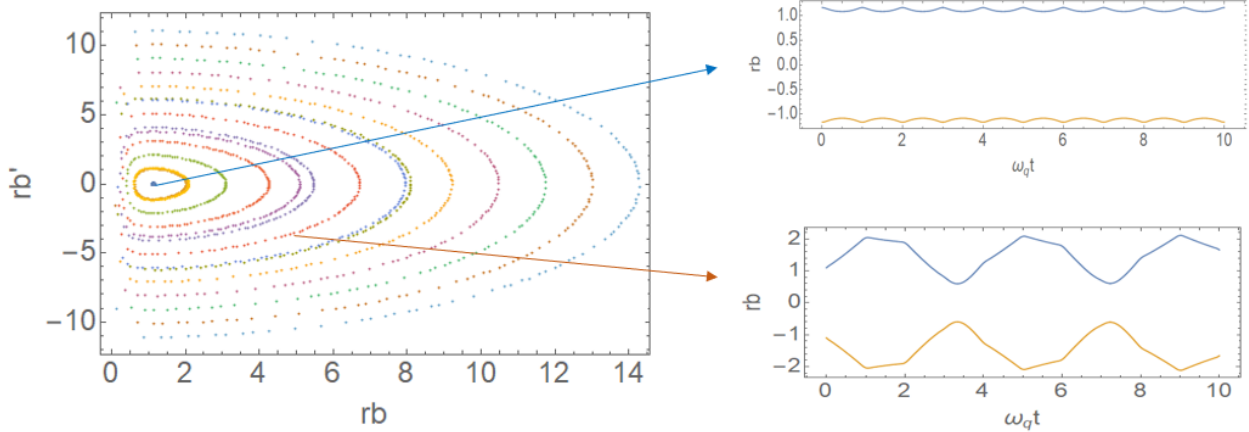


Figure 1: Envelope oscillations on phase plane of $r_b - r'_b$. The values of parameters correspond to $K = 0, \eta = 1/6, \kappa_z(0) = 3.79(\sigma_0 = 45.5^\circ)$. A fixed point on the phase space shows a periodic solution in which initial conditions are $r_b(0) = 1.16, r'_b(0) = 0$. Around the fixed point, there are infinite number of invariant tori having stable betatron oscillations.

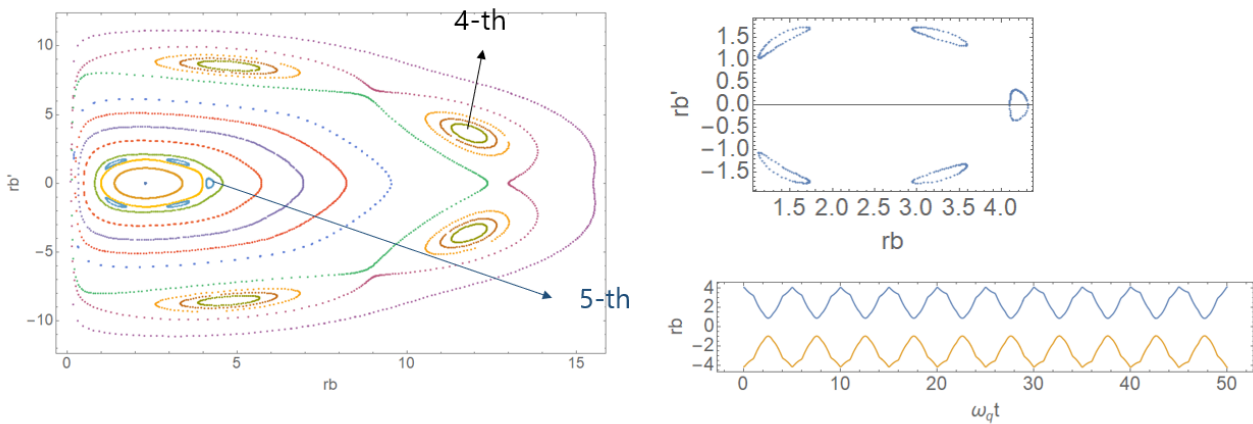


Figure 2: Envelope oscillations on phase plane of $r_b - r'_b$. The values of parameters correspond to $K = 3, \eta = 1/6, \kappa_z(0) = 3.79(\sigma_0 = 45.5^\circ)$. The 5th order resonance corresponds to the five elliptical regions in the vicinity of the fixed point and it has betatron wave number of $2\pi/5$.

For symmetric case with $\sigma_x = \sigma_y = \sigma_r/\sqrt{2}$ in Eq.(6), the space charge term in Eq.(5) becomes $F_{sc,r} = 2 \frac{1-e^{-r/\sigma_r^2}}{r}$.

First, the radial motions of particles in the symmetric Gaussian beams are shown in Fig. 4. For zero perveance, they have uniform and stable oscillations. For $K=3$ and tune depression $\eta \equiv \frac{\sigma}{\sigma_0} = 0.26$, phase space in Fig. 5 shows a region of two concentric curves centered on the fixed points symmetrically located on the x axis. This kind of orbits can be also seen in the resonant motions of mis-matched core and test particles in the uniform density beam under a continuous focusing field [1]. And outside the outer separatrix, particles form quasi-elliptical trajectories. Figure 6 is in different parameters with 60 or 90 degrees of phase advance. There's a similar separatrix symmetrically located on the x axis around a center. But outside region, many other resonant trajectories appear as the distance from the center increases.

For more detailed analysis of the Fig. 6, we expand the exponential part of $F_{sc,r}$ in Eq.(5) by using the Taylor expansion. If we just keep the linear and 2nd order terms, the 4-th order resonance between the matched core (e.g. $\sigma_{env} = 360^\circ$) and test particles can be generated when the phase advance of the particle is about 90° (e.g. $\sigma = 90^\circ$) [21, 22]. The first figure of Fig. 7 shows the 4-th order resonance around the center of the phase plane. If we add the higher order terms more and more (see middle and last figures in Fig. 7), we can see similar trajectories near the center but more resonances are generated as distance increases and become closer to the Fig. 6.

Next, in the case of non-zero canonical momentum under solenoidal focusing field, we have to solve the coupled equations of motion [Eq.(3) and (4)] to see particle motions in real frame. Figure 8 shows the trajectories of many test particles plotted in x-y phase plane with the scale of matched beam radius. A black circle with radius 1 on the x-y plane is

Content from this work may be used under the terms of the CC BY 3.0 licence (© 2018). Any distribution of this work must maintain attribution to the author(s), title of the work, publisher, and DOI.

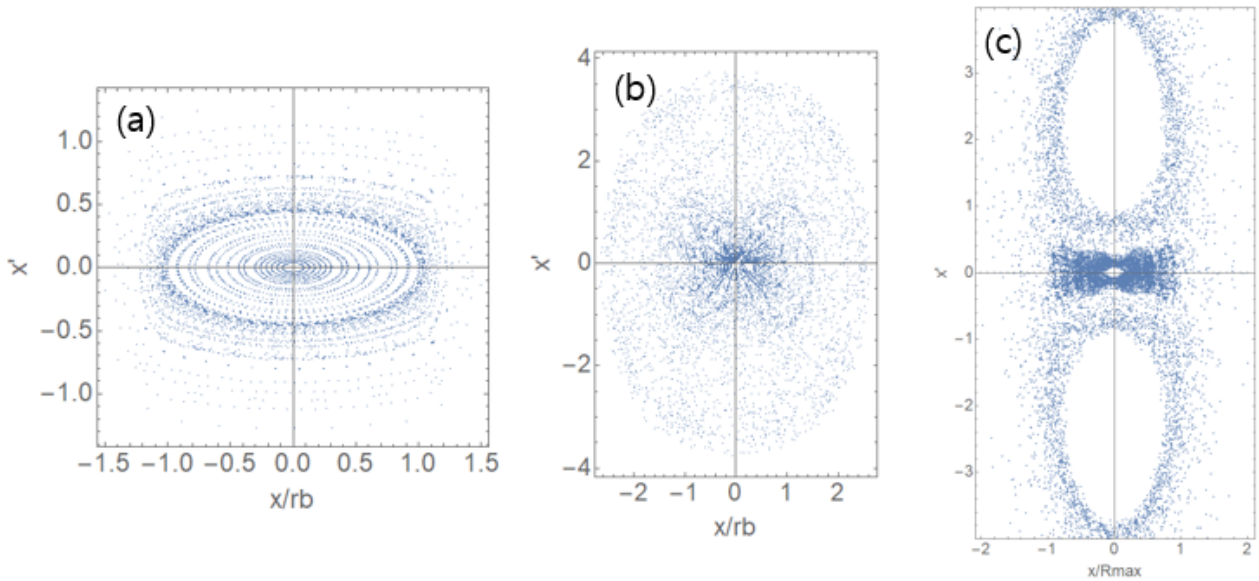


Figure 3: Test particle trajectories of uniform density beams. The corresponding parameters are $K = 3$ and (a) $\sigma_0 = 45.5^\circ$, (b) $\sigma_0 = 45.5^\circ$, (c) $\sigma_0 = 45.5^\circ$. Beam core oscillation is in matched, mis-matched, and the 5th order parametric resonance condition, respectively.

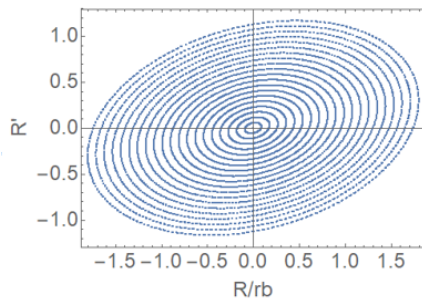


Figure 4: Test particle trajectories of the symmetric Gaussian charge density beam. The corresponding parameters are $K = 0$, $\sigma_0 = 45.5^\circ$, $\sigma = 45.5^\circ$.

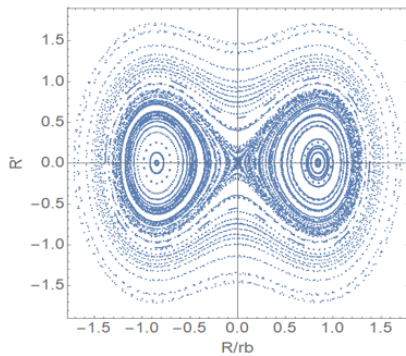


Figure 5: Test particle trajectories of the symmetric Gaussian charge density beam. The corresponding parameters are $K = 3$, $\sigma_0 = 45.5^\circ$, $\sigma = 12^\circ$.

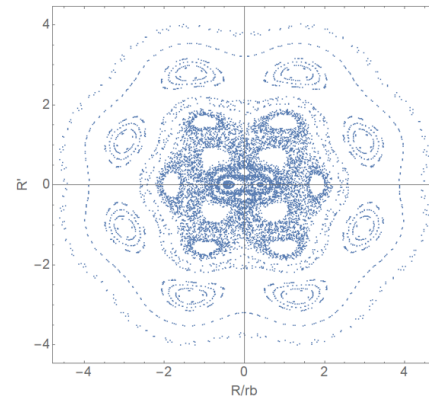


Figure 6: Test particle trajectories of the symmetric Gaussian charge density beam. The corresponding parameters are $K = 2.3$, $\sigma_0 = 115^\circ$, $\sigma = 90^\circ$.

the envelope boundary of the beam. For a detailed study of the test particle motions, let's see a single particle motion. When a single particle is initially loaded within the beam boundary (see Fig. 9), it takes the chaotic orbits that lead to the escape of particle from the beam interior to outside. But as you can see in (c), at very close to the beam boundary, charged particles doesn't go inside the region at which they initially loaded. When a single particle is initially distributed outside the beam boundary (see Fig. 10), it also doesn't go inside the beam interior and doesn't go farther than the particles of Fig. 9. They have chaotic trajectories around the region where they first are.

Test particle orbits can take different kinds of chaotic trajectories depending on the different classes of initial con-

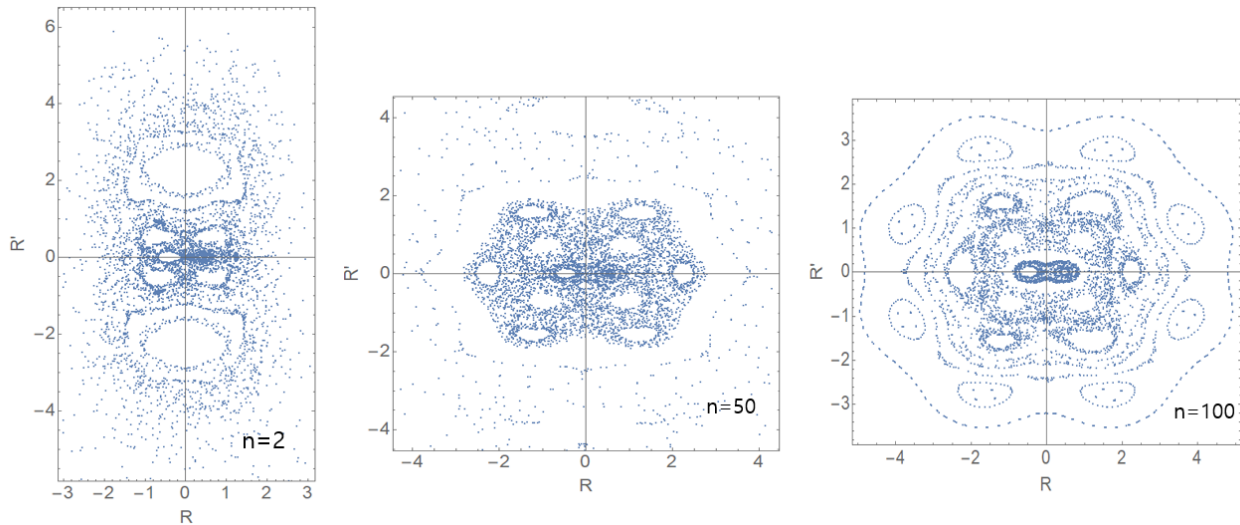


Figure 7: Test particle trajectories of the symmetric Gaussian charge density beam by using Taylor expansion of the exponential part in the space charge force. The corresponding parameters are $K = 2.3$, $\sigma_0 = 115^\circ$, $\sigma = 90^\circ$. (First) $n \leq 2$ terms generate 4-th order resonance around the center. And add the higher order terms (middle) $n \leq 50$, (last) $n \leq 100$.

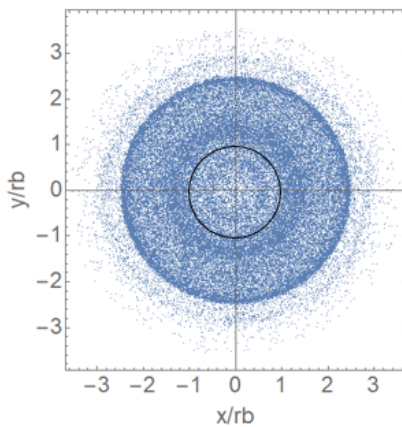


Figure 8: By solving the coupled equations of motion, many test particles are plotted in x - y phase plane with the scale of matched beam radius rb .

ditions in phase space. They can take orbit that is chaotic but stays confined within the outer beam boundary and also leads to the escape of particles from the beam interior to outside, which can become halo particles. When the inside particles go closer to the beam boundary, it tends to be accelerated by the space charge force and resonated with the vibrating beam core so that they can get energy to go farther and make halos.

CONCLUSION

In the high-intensity charged particle beam dynamics, the space charge effects are one of big considerations in terms of the beam emittance growth and halo formations during the beam transportation. Even though the space charge force is linear in the uniform charge density (K-V beam), there can be

a mis-matched core motions because of the initial mismatch. Then the unstable oscillations of the core can generate resonances with the test particles, which can be described by using the particle-core model simulations. Especially under the periodic solenoid magnetic field, the higher order envelope resonances are also generated. For non-uniform charge density beams (Gaussian), the space charge force is non-linear so that it affects the particle motions even though the core is matched. To see the non-linear effects on the halo formations, we solved the radial (in the case of symmetric Gaussian beam) and coupled equations of motion with many test particles and a single particle motion. The particle-core model doesn't consider the self-consistency that can be achieved only from the Particle-In-Cell (PIC) simulations. Moreover, there's no longitudinal effects of the space charge force and acceleration. So we can study further by including those additional effects on the beam dynamics and apply to the design of the halo and beam loss diagnostics.

REFERENCES

- [1] T. P. Wangler, "Particle-core model for transverse dynamics of beam halo", *Phys. Rev. Accelerators and Beams*, vol. 1, no. 9, 1998.
- [2] Q. Qian, R. C. Davidson, C. Chen, "Chaotic particle motion and halo formation induced by charge nonuniformities in an intense ion beam propagating through a periodic quadrupole focusing field", *Physics of Plasmas*, vol.2 no. 7, pp.2674–2686, 1995.
- [3] Q. Qian, R. C. Davidson, C. Chen, "Halo formation induced by density nonuniformities in intense ion beams", *Phys. Rev. E*, vol. 51, no. 6, p. R5216, 1995.
- [4] I. Hofmann, "Performance of solenoids versus quadrupoles in focusing and energy selection of laser accelerated protons",

Content from this work may be used under the terms of the CC BY 3.0 licence © 2018). Any distribution of this work must maintain attribution to the author(s), title of the work, publisher, and DOI.

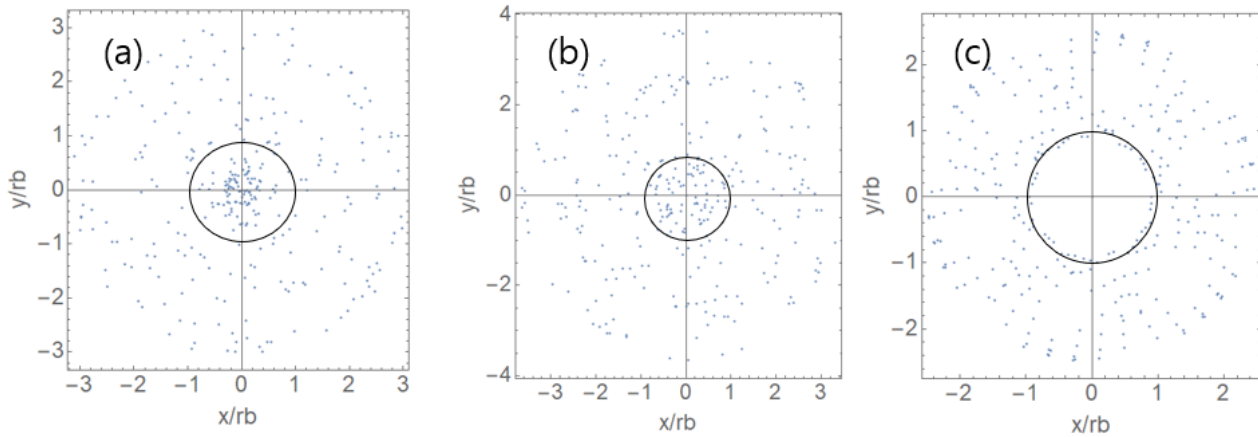


Figure 9: A single particle motion of Fig. 8, with different initial conditions. A particle is initially loaded outside the beam boundary (a black circle) which are (a) $(\frac{x}{r_b})^2 + (\frac{y}{r_b})^2 = (0.1)^2$, (b) $(\frac{x}{r_b})^2 + (\frac{y}{r_b})^2 = (0.7)^2$, (c) $(\frac{x}{r_b})^2 + (\frac{y}{r_b})^2 = (0.9)^2$.

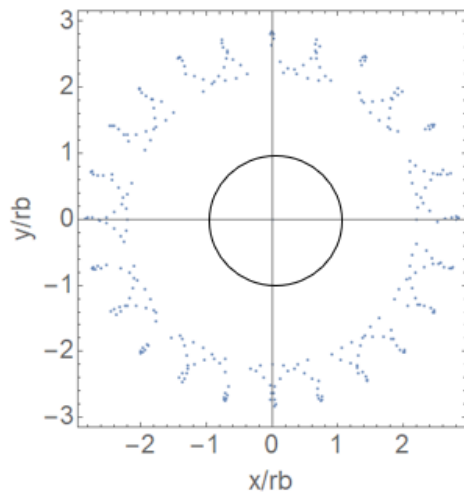


Figure 10: A single particle motion of Fig. 8, with different initial conditions. A particle is initially loaded inside the beam boundary (a black circle) which is $(\frac{x}{r_b})^2 + (\frac{y}{r_b})^2 = (2.2)^2$.

Phys. Rev. Accelerators and Beams, vol. 16, no. 4, p. 041302, 2013.

- [5] C. Chen, R. C. Davidson, “Nonlinear resonances and chaotic behavior in a periodically focused intense charged-particle beam”, *Phys. Rev. Lett.*, vol. 72, p. 14, p. 2195, 1994.
- [6] R. C. Davidson, H. Qin, “An introduction to the physics of intense charged particle beams in high energy accelerators”, World Scientific, 1994.
- [7] I. M. Kapchinskij, V. V. Vladimirkij, “Limitations of proton beam current in a strong focusing linear accelerator associated with the beam space charge”, in *Proc. HEACC 1959*, Geneva, Switzerland, Sep. 1959, pp.274–287.
- [8] R. C. Davidson, “Physics of nonneutral plasmas”, *World Scientific Publishing Company*, 2001.
- [9] M. Reiser, “Theory and design of charged particle beams”, *John Wiley & Sons*, 2008.
- [10] I. Hofmann, “Space Charge Physics for Particle Accelerators”, *Springer*, 2017.
- [11] J. M. Struckmeier, J. Klabunde, “On the stability and emittance growth of different particle phase-space distributions in a long magnetic quadrupole channel”, *Part. Accel.*, vol. 15, pp.47–65, 1984.
- [12] A. Pathak, S. Krishnagopal, “Higher order mode beams mitigate halos in high intensity proton linacs”, *Phys. Rev. Accelerators and Beams*, vol. 20, no. 1, p. 014201, 2017.
- [13] G. Franchetti, I. Hofmann, D. Jeon, “Anisotropic free-energy limit of halos in high-intensity accelerators”, *Phys. Rev. Lett.*, vol. 88, no. 25, p. 254802, 2002.
- [14] F. Gerigk, “Beam halo in high-intensity hadron accelerators caused by statistical gradient errors”, *Phys. Rev. Accelerators and Beams*, vol. 7, no. 6, p. 064202, 2004.
- [15] J. S. O’Connell, “Beam halo formation from space-charge dominated beams in uniform focusing channels”, in *Proc. PAC’93*, pp. 3657-3659, 1993.
- [16] T. F. Wang, “Particle-core study of halo dynamics in periodic-focusing channels”, *Phys. Rev. E*, vol. 61, no. 1, p. 855, 2000.
- [17] J. Qiang, R. D. Ryne, “Beam halo studies using a three-dimensional particle-core model”, *Phys. Rev. Accelerators and Beams*, vol. 3, no. 6, p. 064201, 2000.
- [18] I. Hofmann *et al.*, “Stability of the Kapchinskij-Vladimirkij (KV) distribution in long periodic transport systems”, *Part. Accel.*, vol. 13, pp. 145-178, 1982.
- [19] M. A. Furman, “Compact complex expressions for the electric field of two-dimensional elliptical charge distributions”, *American Journal of Phys.*, vol. 62, no. 12, pp.1134–1140, 1994.
- [20] G. Stupakov, P. Gregory, “Classical Mechanics and Electromagnetism in Accelerator Physics”, *Grad. Texts Math.*, 2018.
- [21] L. Groening *et al.*, “Experimental observation of space charge driven resonances in a linac”, in *Proc. LINAC’10*, Tsukuba, Japan, Sep. 2010, paper TH303.
- [22] D. Jeon, L. Groening, G. Franchetti, “Fourth order resonance of a high intensity linear accelerator”, *Phys. Rev. Accelerators and Beams*, vol. 12, no. 5, p. 054204, 2009.